INTERNATIONAL JOURNAL OF HYDROGEN ENERGY 46 (2021) 8329–8343

Available online at www.sciencedirect.com

ScienceDirect

journal homepage: www.elsevier.com/locate/he

Quantitative risk assessment using a Japanese hydrogen refueling station model

Tomoya Suzuki [a], *Kento Shiota* [b], *Yu-ichiro Izato* [c], *Masahiro Komori* [d], *Koichi Sato* [d], *Yasuyuki Takai* [d], *Takayuki Ninomiya* [d], *Atsumi Miyake* [b,*]

[a] *Graduate School of Environment and Information Sciences, Yokohama National University, 79–7 Tokiwadai, Hodogaya–ku, Yokohama, Kanagawa 240–8501, Japan*

[b] *Institute of Advanced Sciences, Yokohama National University, 79–5 Tokiwadai, Hodogaya–ku, Yokohama, Kanagawa, 240–8501, Japan*

[c] *Faculty of Environment and Information Sciences, Yokohama National University, 79–7 Tokiwadai, Hodogaya–ku, Yokohama, Kanagawa, 240–8501, Japan*

[d] *Japan Petroleum Energy Center, 2–11–1 Shibakoen, Minato–ku, Tokyo, 105–0011, Japan*

HIGHLIGHTS

- A model representing Japanese hydrogen refueling stations under current Japanese laws and regulations was constructed.
- A quantitative risk assessment of the model was conducted.
- This assessment visualized individual risks of the hydrogen refueling station model.
- Jet fire risks are the highest contribution to the individual risks in the outside of the station.

ARTICLE INFO

Article history:
Received 16 September 2020
Received in revised form
15 November 2020
Accepted 5 December 2020
Available online 25 December 2020

Keywords:
Quantitative risk assessment
Hydrogen refueling station
Individual risk
Jet fire

ABSTRACT

Although hydrogen refueling stations (HRSs) are becoming widespread across Japan and are essential for the operation of fuel cell vehicles, they present potential hazards. A large number of accidents such as explosions or fires have been reported, rendering it necessary to conduct a number of qualitative and quantitative risk assessments for HRSs. Current safety codes and technical standards related to Japanese HRSs have been established based on the results of a qualitative risk assessment and quantitative effectiveness validation of safety measures over ten years ago. In the last decade, there has been much development in the technologies of the components or facilities used in domestic HRSs and much operational experience as well as knowledge to use hydrogen in HRSs safely have been gained through years of commercial operation. The purpose of the present study is to conduct a quantitative risk assessment (QRA) of the latest HRS model representing Japanese HRSs with the most current information and to identify the most significant scenarios that pose the greatest risks to the physical surroundings in the HRS model. The results of the QRA show that the risk contours of 10^{-3} and 10^{-4} per year were confined within the HRS boundaries, whereas the risk contours of 10^{-5} and 10^{-6} per year are still present outside the HRS. Comparing the breakdown of the individual risks (IRs) at the risk ranking points, we conclude that the risk of jet fire demonstrates the highest contribution to the

* *Corresponding author.*
E-mail address: miyake-atsumi-wp@ynu.ac.jp (A. Miyake).

https://doi.org/10.1016/j.ijhydene.2020.12.035

risks at all of the risk ranking points and outside the station. To reduce these risks and confine the risk contour of 10^{-6} per year within the HRS boundaries, it is necessary to consider risk mitigation measures for jet fires.

1. Introduction

Hydrogen is widely considered to be a clean source of energy in terms of carbon dioxide emission reduction. In the near future, hydrogen infrastructures for the commercialization of fuel cell vehicles (FCVs) will be developed. Hydrogen refueling stations (HRSs) are essential for the operation of FCVs and have become widespread in Japan. The development of HRS started in 2013 in Japan, and various types of HRSs have been constructed and commercialized. There are 135 stations in operation as of today. The Ministry of Economy, Trade, and Industry in Japan has set a numerical target for HRSs of approximately 320 in 2025 and approximately 900 in 2030 [1]. Therefore, it is expected that the social implementation and dissemination of HRSs will continue to accelerate toward the state in which many citizens can use hydrogen energy.

Compared with other fossil fuels, hydrogen has advantages in terms of reducing carbon dioxide emissions and improving energy security in Japan. On the other hand, hydrogen also has hazards, such as hydrogen embrittlement, explosiveness, and flammability. In addition, since hydrogen has a relatively wide explosive range and low minimum ignition energy, which is approximately one-tenth that of gasoline, the use of hydrogen can easily result in explosions or fires by ignition after leakage. A large number of accidents (hydrogen release, explosions, or fires) have been reported in accident databases such as Hydrogen Incident and Accident Database [2]. A large-scale leak, fire, and explosion of hydrogen occurred in Sandvika, Norway, on June 10th, 2019, and two people were injured [3]. For these reasons, a number of qualitative and quantitative risk assessments for HRSs have been conducted.

Qualitative risk assessment is often conducted with accidental scenario identification using process hazard analysis methods. This is one of the most important aspects of risk assessment because the scenarios are necessary to examine and propose risk mitigation measures. For off-site or on-site HRSs, there have been several studies on qualitative risk assessments using hazard identification methods such as Hazard and Operability (HAZOP) studies or Failure Mode and Effect Analysis (FMEA) [4–7], and risk evaluation methods, such as risk matrices [8–10].

On the other hand, quantitative risk assessments (QRAs) have also been conducted for HRSs. Quantitative risk assessment is one of the tools that are used in risk-informed decision making for the determination of safety distances, risk reduction measures, and land-use planning around activities in which hazardous materials are involved. In order to estimate quantitative risks, it is necessary to estimate the frequencies and consequences of risk scenarios, respectively.

Frequency analyses for HRSs have a significant problem in that there is insufficient statistical data for failure frequencies because HRSs have been only used for a short period throughout the world, although the data should be used in the analyses. Therefore, the frequencies were estimated from other chemical plants in the past. However, one of the approaches to solve this problem is to use Bayes' theorem. Theoretically, Bayes' theory can estimate the frequency from limited statistical frequency data, and is a powerful tool for estimating the failure frequency for systems like HRSs, it is therefore becoming a mainstream approach. LaChance et al. [11] estimated the failure frequencies of a variety of components (pipes, flanges, or valves, etc.) consisting of the HRS process from a lot of data sources of hydrocarbons as a prior distribution in combination with scarce actual hydrogen data. Then, they added the failure frequency data for other components (instruments, etc.) to this dataset [12]. There are other examples of frequency analysis in the risk assessment of an organic hydride HRS using a Bayesian approach [13]. In addition, static or dynamic Bayesian network has been used as a method for estimating the frequency of occurrence of scenarios [14,15]. There are other research examples related to frequency analysis that focuses on the probability of human error in HRSs [16].

Related to the consequence analysis of HRSs, numerous experiments to develop an analytical and numerical model for the prediction of accidental phenomena, such as hydrogen diffusion, vapor cloud explosions (VCE), or jet fires, have been carried out. Many studies have modeled hydrogen diffusion or explosion by computational fluid dynamics (CFD) [17–21]. In addition, regarding jet fires involving hydrogen, a large number of experimental examples, including low to high-pressure conditions, numerical model development, and evaluation of flame length and radiation heat flux have been reported [22–26]. At present, research on understanding the phenomenon of cryogenic hydrogen jet fires is also being carried out [27]. In addition, quantitative consequence analysis has been conducted for effective validation of risk mitigation measures suggested by considering the various scenarios [28]. Simulation software to support the consequence analysis for HRSs such as the FLame ACceleration Simulator (FLACS), the Process Hazard Analysis Software Tool (PHAST), and the Hydrogen Risk Assessment Model (HyRAM) have been developed.

Combined with these analyses, a number of QRAs have been reported. Matthijsen et al. [29] obtained safety distances for a compressed HRS using quantitative risk and compared the obtained values to those for a gas station, a compressed natural gas refueling station, and a liquefied petroleum gas refueling station. LaChance et al. [30,31] proposed an

approach for the risk-informing permitting process for HRSs using QRA techniques to establish a more reasonable safety distance. Zhiyong et al. [32,33] conducted QRAs for various types of compressed HRSs and discussed safety distances. Gye et al. [34] conducted a QRA for an HRS in an urban area.

Current safety codes and technical standards related to Japanese HRSs have been established based on the results of a risk assessment implemented as a part of the ''Establishment of Codes & Standards for Hydrogen Economy Society – Study on the Safety Technologies of Hydrogen Infrastructure'' conducted by the New Energy and Industrial Technology Development Organization (NEDO) from 2005 to 2009. This work identified the risk scenarios for a compressed and liquefied HRS model, assessed the risks of the scenarios using a qualitative method, and quantitatively verified the effectiveness of the safety measures [8,9,28]. In the last decade since this risk assessment, there has been much development in the technologies of the components or facilities used in domestic HRSs and much operational experience as well as knowledge to use hydrogen in HRSs safely have been gained through years of commercial operation. Therefore, it is necessary to conduct a QRA with the most current information on HRS technology and to update the QRA results before the number of stations become more widespread.

The purpose of the present study is to conduct a QRA of an HRS model representing Japanese HRSs to include the most current information and to identify the most significant scenarios that pose the greatest risks to the physical surroundings in the HRS model. Section Quantitative risk assessment describes the HRS model and the QRA methodology used in this study. We selected a compressed HRS, which is an off-site station, as the model because it includes the common processes for all the HRSs. Section Results and discussion describes the results of the QRA, which are the individual risks of the scenarios combined with the consequences and frequencies thereof, and discusses the most significant scenarios. Finally, Section Conclusion presents the conclusions of this study.

2. Quantitative risk assessment

2.1. Methodology

A QRA is a valuable tool for determining the risk and supporting decision making. The QRA methodology was published by the Center for Chemical Process Safety in their Guidelines for Chemical Process Quantitative Risk Analysis [35] and by the Dutch Government in their Guidelines for QRA, known as the Nederlandse Organisatie voor Toegepast Natuurwetenschappelijk Onderzoek (TNO) Purple Book [36]. Det Norske Veritas-Germanischer Lloyd (DNV-GL) performed a systematic review of QRA examples for HRSs and reported a methodology based thereon [37]. Therefore, in the present paper, we conducted a QRA (Fig. 1) based on this report and the concrete contents of each step were based on the TNO Purple Book because a 'full QRA' can be conducted [38].

The first step is to define the HRS model, including adequate data for conducting a QRA. We defined the HRS model expected to be widely used in the near future. The second step is to identify hazards and select accidental scenarios, such as hydrogen leakage from components causing jet fires, flash fires, or VCEs. The third step is to analyze risks, including frequency assessment, consequence and impact assessment, and risk expression. The frequencies of these scenarios are estimated using event tree analysis (ETA) by giving the initial event frequencies and individual branch probabilities. Consequences, such as radiation heat flux from jet fires or flash fires or overpressure from VCEs, are calculated by some analytical models of final events. Impacts that were only considered to be lethality were assessed in the present study. The fourth step is to estimate risks by combining the frequencies and impacts. In the present study, we estimated individual risk (IR), which is the frequency of an individual dying due to loss of containment events and is usually indicated as a risk contour around the facilities. The final step is to compare the obtained risk with acceptance criteria, which were herein adopted from the ISO 19880-1, which defines such as the installation and operation for the safety for compressed HRS [39]. According to the ISO 19880-1, the average IR for vulnerable external populations and for facility users and workers should not exceed 10^{-6} per year and 10^{-4} per year, respectively.

In the present study, PHAST 8.11 and Safeti 8.11 from DNV-GL were used to support QRA. The PHAST allows for analysis of process hazards and consequences (e.g. fire events and explosions) using various prediction model equations based on the physical parameters. Safeti allows a QRA to be conducted by combining the results obtained from the PHAST and the frequency of events obtained from ETA. The features of Safeti are such that it is possible to conduct a QRA for a large number of scenarios, and the risks can be visualized as risk contours. The effectiveness of the PHAST and Safeti are widely ensured for petrochemical plants or other chemical plants, and there are a number of studies on hydrogen-related facilities and HRSs.

2.2. Description of the hydrogen refueling station model

In order to conduct a risk assessment, it is important to clarify how to define models of systems and processes to be considered because risk assessment is just conducted based on the models, and other elements that are not included in the models are not considered. We defined an HRS model that has installations and components that represent Japanese HRSs and that does not have particular equipment or features. In addition, we defined an HRS model that minimizes the station area under current Japanese laws and regulations because the conservative assessment is possible by setting the conditions where the risk contours easily spread outside the station. Therefore, we tried to ensure the generality of the model by information based on the configuration of the components, the layout of existing stations, and interviews with related companies. Furthermore, we also tried to ensure that the

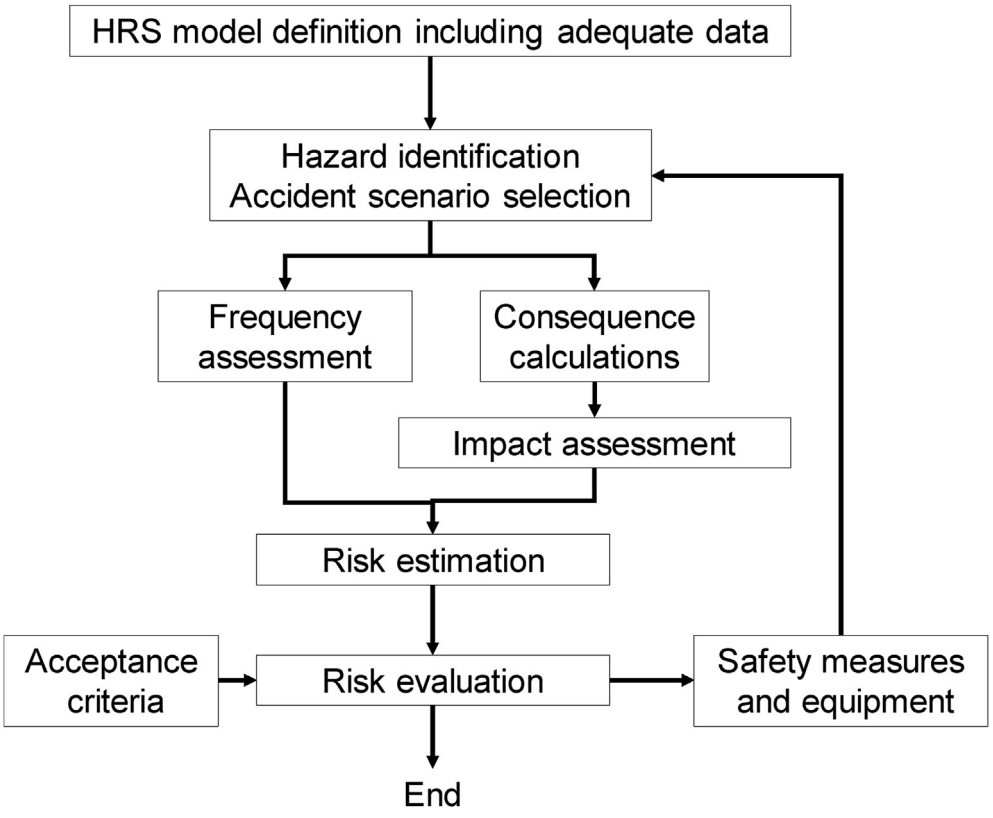

Fig. 1 – Procedure of quantitative risk assessment.

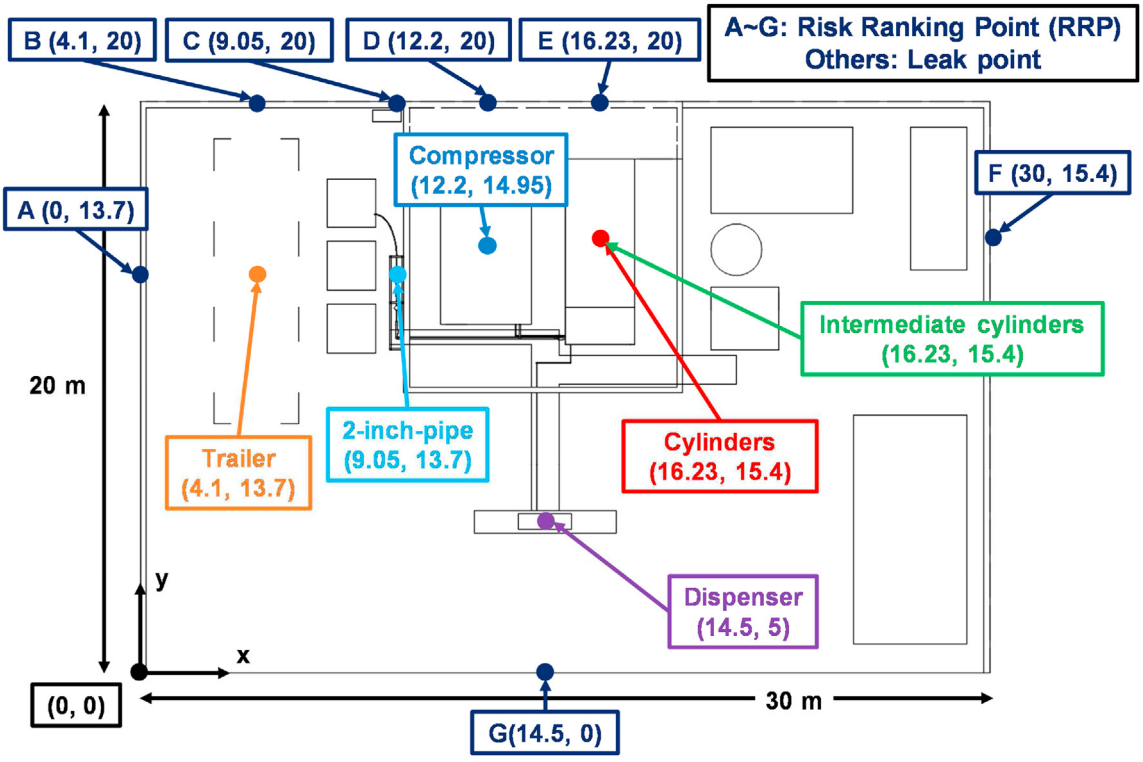

Fig. 2 – Hydrogen refueling station layout model with representative leakage points for each node and risk ranking points.

model had adequate information for conducting a QRA, such as the station layout and the piping and instrumentation diagram (P&ID).

2.2.1. *Station layout*

Fig. 2 shows the layout of the HRS model and depicts the location of the main nodes. There are some nodes that may leak hydrogen, namely, the Trailer, 2-inch-pipe, Compressor, Intermediate cylinders, Cylinders, and Dispenser nodes. Some other facilities, such as an office, a chiller for cooling hydrogen, and a utility facility, are included in the model. However, how these 3D structures can affect the risks is not considered. Although hydrogen leakage can occur at various points in these nodes, we defined the representative leak points at each node. For example, the representative point for the Trailer node was defined at the center of its parking space. Similarly, the leak points for other nodes were defined as the center of each node. We also defined seven risk ranking points (RRPs), which represents the points at which the risks for the HRS are evaluated, on the HRS boundary and nearest each representative leak point for evaluating the risks.

2.2.2. *Piping and instrumentation diagram*

Fig. 3 shows the P&ID for the HRS process model and the legend for the components. The hydrogen supplied from an external source is transported to the station by the hydrogen trailers. There are two connectors for providing the hydrogen at 19.6 MPa and 45 MPa, respectively. The pressure of the hydrogen is reduced to 0.6 MPa through a pressure reducing valve and 2-inch pipes and is then increased to 82 MPa by the compressor to store hydrogen in the cylinders. The flow rate for the compressor is 340 Nm^3/h, which is maintained at a constant value, regardless of the pressure at the inlet and outlet sides, by providing the inlet pressure at the constant value (0.6 MPa). Five intermediate cylinders as the gas source of the compressor are provided. In order to efficiently fill the FCV with hydrogen, three cylinders (1st, 2nd, and 3rd bank) are used. The dispenser charges hydrogen to the FCV tank, which is filled with hydrogen from 10 MPa to 80 MPa in approximately 3 min.

2.2.3. *Components and safety equipment*

In the P&ID, there are various types of components, such as cylinders, valves, and pipes. The number of the components and the pipe length, which are needed to analyze the frequencies of accident scenarios and the risks, are estimated by examining the P&ID. The list of nodes and the number of components are provided in Table 1. The inner diameter of the pipe for high-pressure hydrogen is defined as 6.3 mm, and that for low-pressure hydrogen (less than 0.6 MPa) is defined as 50.5 mm. There are components not only for normal operation but also for safety.

2.3. *Hazard identification and accident scenario selection*

Each accident scenario occurring in an HRS, such as hydrogen leakage, is a result of various hazards, for example, pipe

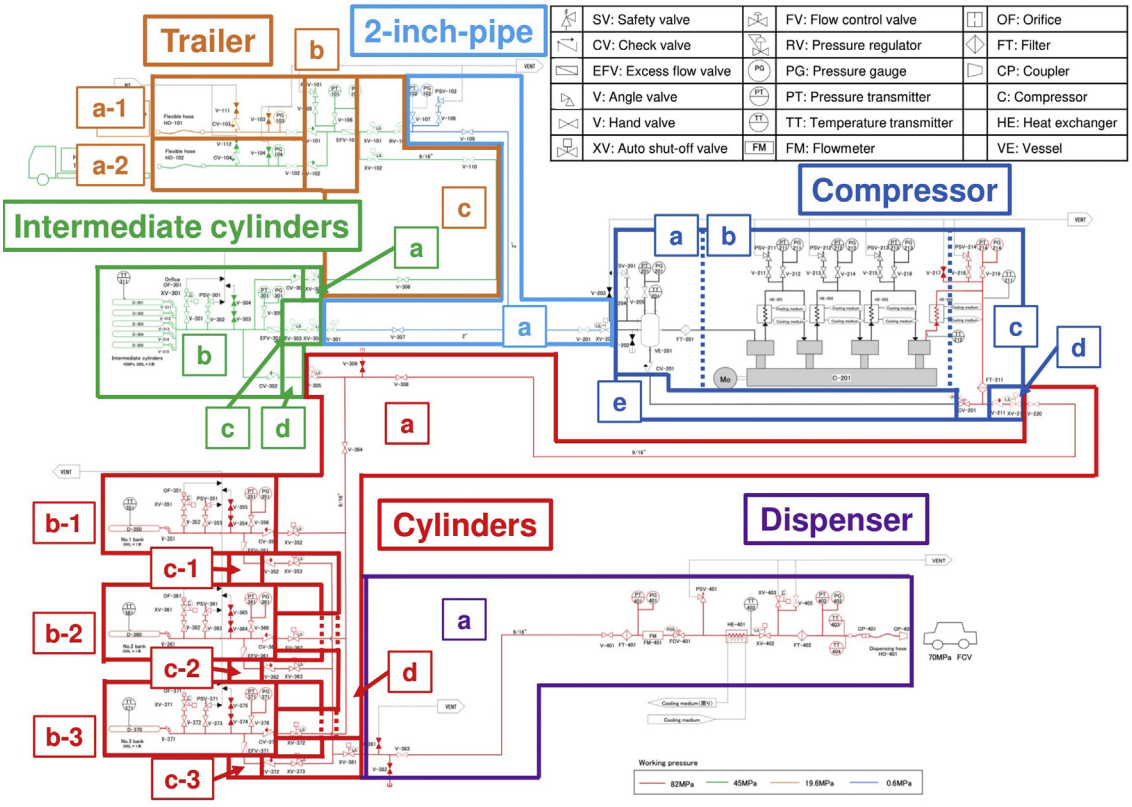

Fig. 3 – Piping and instrumentation diagram (P&ID) and nodes for hydrogen refueling process.

Table 1 – Number of components in each node.

Node		Trailer			2-inch-pipe	Intermediate cylinders				Compressor						Cylinders			Dispenser
Component	Unit	a-1 a-2	b	c	a	a	b	c	d	a	b	c	d	e	a	b-1 b-2 b-3	c-1 c-2 c-3	d	a
Compressors	–	0	0	0	0	0	0	0	0	0	1	0	0	0	0	0	0	0	0
Cylinders	–	0	0	0	0	0	5	0	0	1	0	0	0	0	0	1	0	0	0
Filters	–	0	0	0	0	0	0	0	0	1	0	1	0	0	0	0	0	0	2
Flanges	–	0	0	0	12	0	0	0	0	0	0	0	0	0	0	0	0	0	0
Hoses	–	1	0	0	0	0	0	0	0	0	0	0	0	0	0	0	0	0	1
Joints	–	3	7	12	4	0	17	0	0	8	20	6	0	2	15	10	0	4	38
Pipes	m	1.74	3.00	14.79	17.37	0.21	10.56	0.55	0.21	0	0	0	0	0	15.22	4.00	0.15	4.12	17.37
Valves	–	4	6	5	8	1	15	2	1	6	10	4	2	0	7	10	0	7	9
Instruments	–	1	2	0	2	0	2	0	0	2	6	2	0	0	0	2	0	0	5

corrosion, valve failure, or a filling hose rupture. In order to conduct hazard identification or accident scenario selection, we divided the P&ID into several nodes. In the present study, all of the components in the P&ID except for the vent lines and the chiller system are included in all nodes. Each node is divided into a number of small nodes at the check valves, the excess flow valves (EFVs), and the auto shut-off valves, so that the parameters dominating hydrogen leakage, namely, inventory, temperature, and pressure, are the same for each node. The results of dividing the nodes are shown in Fig. 3. Then, we conducted HAZOP and FMEA to identify hazards and selected scenarios involving hydrogen leakage caused by damage or failure of components in the process.

After hydrogen leakage, some final events, namely, jet fires, flash fires, and VCEs, can occur [11]. They are determined by hydrogen leak duration and ignition time. If a large amount of hydrogen leakage caused by pipe rupture occurs, then the EFV located upstream from the leak point will operate. There are some locations in the process at which EFVs are not operated when a hydrogen leak occurs. Therefore, two event trees are considered in which EFVs are operated and not operated (Figs. 4 and 5). Fig. 4 described the event progress of leaks when the leak occurs within the operating range of the EFV, while Fig. 5 described the event progress of the other leaks. It is assumed that the EFV takes 0.1 s from the start of the leak to the end of the leak because this valve works rapidly [40]. In the case of immediate ignition, it is assumed that flash fires will occur as the final event because the released amount of hydrogen is small, whereas it is assumed that no effect occurs when the hydrogen does not ignite. For other leaks, the

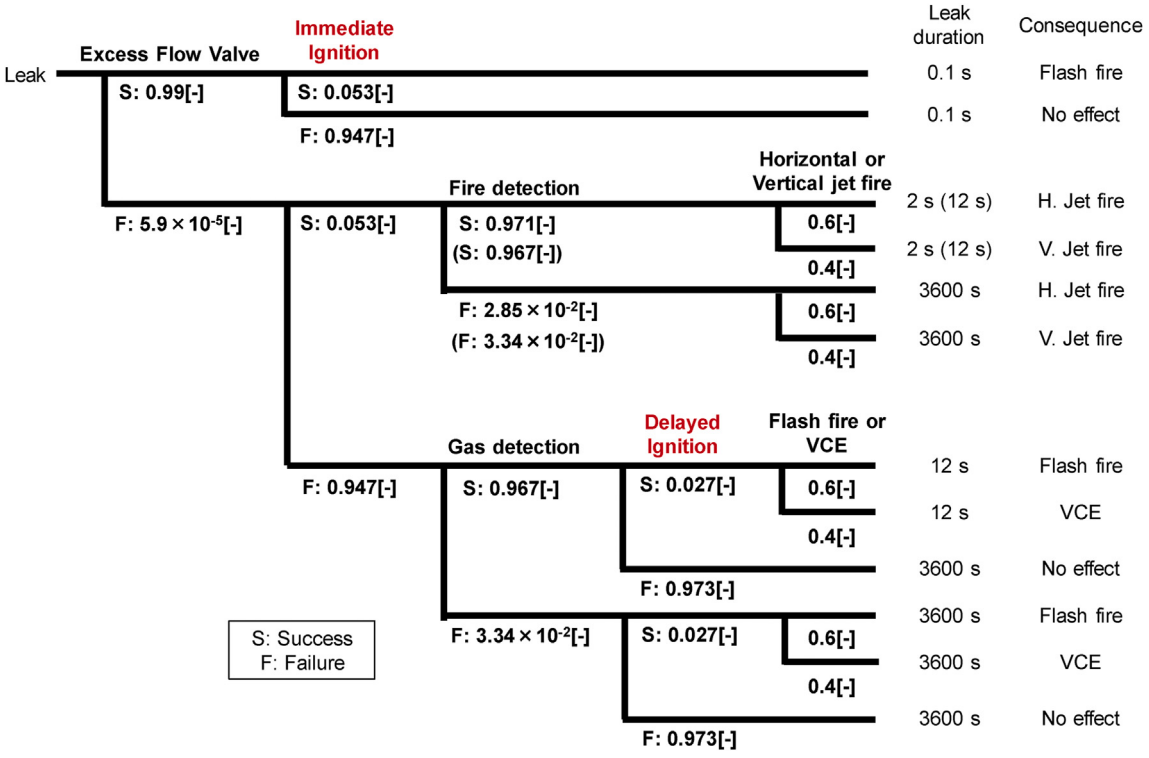

Fig. 4 – Event tree beginning from hydrogen leak.

auto shut-off valves are operated by signals from the gas detector and the flame detector, rather than operating the EFVs, because EFVs are only effective for large leaks. When the hydrogen leakage is immediately ignited and a jet fire occurs, it is assumed that the time from the beginning to the end of the leak by detecting the flame and operating the auto shut-off valve is 2 s. On the other hand, the jet fire will continue if the flame detection fails. Two types of jet fires, horizontal and vertical, are assumed to occur based on the leak direction. If the leak continues without immediate ignition, then the leaked hydrogen disperses into the atmosphere, and the gas detector will detect hydrogen. According to information provided by companies developing gas detectors, it takes 9 s from the start of leakage to hydrogen detection and 3 s to complete closure of the auto shut-off valve completely. Therefore, it takes 12 s from the start of leakage until the leakage is stopped. In the present study, it is assumed that both gas detectors and flame detectors take 12 s to stop hydrogen leakage and that the risks of jet fires are evaluated conservatively because both effects are modeled simultaneously. If delayed ignition occurs after hydrogen leakage for 12 s, VCEs or flash fires are expected to occur as final events. In the case that ignition does not occur, hydrogen diffuses into the atmosphere but there is no effect. If all safety equipment fails, then the hydrogen will continue to leak, and jet fires will occur by immediate ignition, and VCEs and flash fires will occur by delayed ignition.

2.4. *Frequency assessment*

Event tree analysis was used to estimate the frequencies of the scenarios. Hydrogen leakage was set as the initiating events, the top event of the event trees, because all of the selected scenarios were caused by hydrogen leakage. Figs. 4 and 5 shows the event tree described in the HRS model. In the present study, the frequencies of hydrogen leakage are regarded as equal to the failure frequencies for components. Sandia National Laboratories reported the failure frequencies for nine types of components existing in the HRS process, namely, compressors, cylinders, filters, flanges, hoses, joints, pipes, valves, and instruments [12]. They also suggested five leak diameters (Rupture, Major, Medium, Minor, and Very Small) for leaks caused by individual component failures, and estimated the frequencies for each leak. Therefore, we identified all the components in the P&ID and defined the frequency of hydrogen leaks as the value described above.

The frequencies of the final events can be calculated by appropriately giving the frequency of the initiating events and branch probabilities. The branches of the ETA are given based on the success or failure of the safety equipment, immediate or delayed ignition, and so on. We used the probability of failure on demand (PFD) of a check valve (5.9×10^{-5} [41]) instead of the PFD of an EFV because there is no credible value for the PFD of an EFV. The PFD of a gas detection system is caused by failure of the sensor, failure of the logic circuit connecting the sensor and operatives, or failure of the auto shut-off valve at the operatives. Therefore, the sum of the PFDs represents the failure probability for the entire system. In addition, it is assumed that there is no failure of the logic circuit. Many gas leak detectors have various types of measurement principles, but some of them cannot be used for hydrogen. For example, contact burning-type gas sensors have been used in the HRS, but, in principle, it is impossible to detect hydrogen with infrared-type gas sensors. Since there is

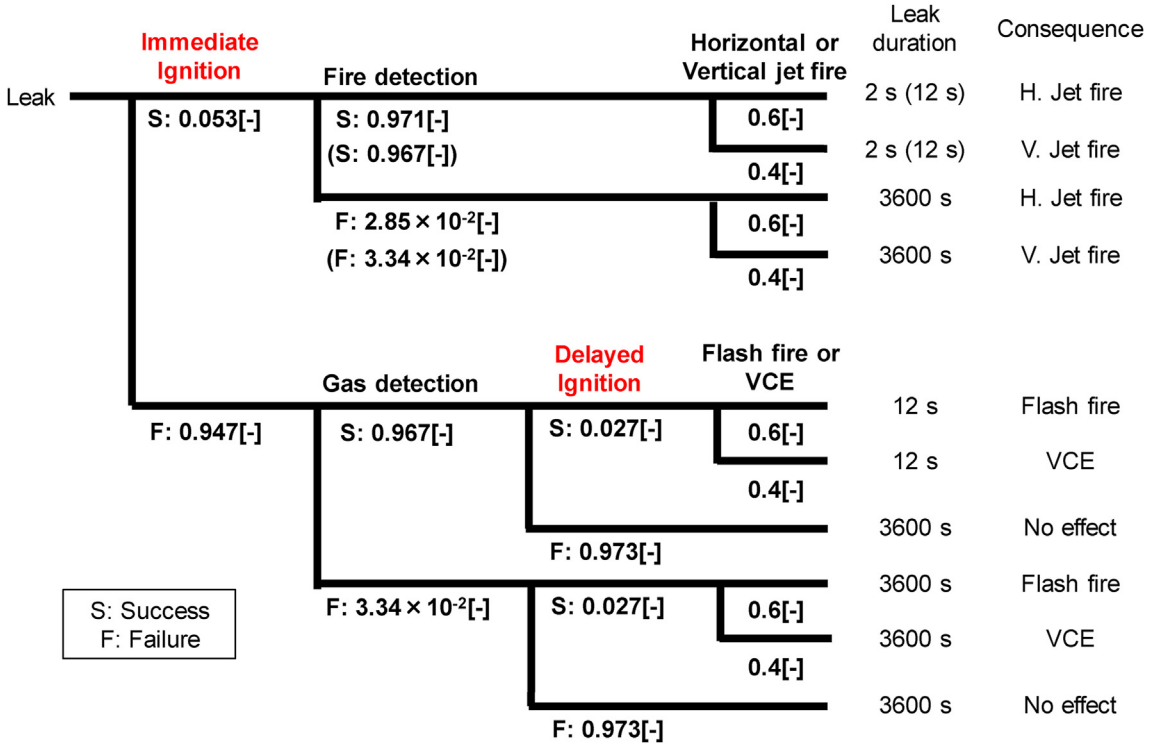

Fig. 5 – Event tree beginning from hydrogen leak.

no credible value for the PFD of a gas leak detector, we estimated the PFD of the detector based on the failure rate of a catalytic fire and gas detectors for hydrocarbon gas ($\lambda = 7.6 \times 10^{-6}$/h [42]). As the operation of the gas leak detector is checked in a periodic inspection once a year (T = 8760 h), the PFD is obtained as follows:

$$PFD_{detect} = \frac{1}{2} \times \lambda \times T = \frac{1}{2} \times \left(7.6 \times 10^{-6}\right) \times 8760 = 3.3 \times 10^{-2}[-]$$

Furthermore, the PFD of the auto shut-off valve is 1.2×10^{-4} [41]. Thus, the PFD of the entire system is obtained as follows:

$$PFD_{entire} = PFD_{detect} + PFD_{shut} = 3.3 \times 10^{-2} + 1.2 \times 10^{-4} = 3.3 \times 10^{-2}[-]$$

The PFD of a flame detection system is 2.9×10^{-2} (calculated in the same manner). In the present study, the leak duration when the auto shut-off valve is operated is regarded as the leak duration by the gas detector, and the PFD of the gas detection system is regarded as the PFD of the gas detector for conservative evaluation.

The ignition probabilities for released hydrogen for each leak rate were also given by Sandia [12]. In the case of immediate ignition, a jet fire can occur as the final event. The branch probability of jet fires was set to 0.6 for the jet fires in the horizontal direction and 0.4 for jet fires in the vertical direction. In the case of delayed ignition, VCEs and flash fires can occur as the final events. The branch probabilities of VCEs and flash fires were set to 0.4 and 0.6, respectively [36].

As a special case, the delayed ignition probability for an FCV refueled with hydrogen as the ignition source was taken into account. Assuming that an FCV arrives at an HRS to refuel with hydrogen per hour, the vehicle will stay for 5 min, and its ignition probability is 0.4, based on an ignition source for gasoline vehicles [36], the ignition probability for the FCV in a parking space is estimated as follows:

$$1/60[/\text{min}] \times 5[\text{min}] \times 0.4[-] = 0.033[-]$$

2.5. Consequence calculations

Table 2 shows the process conditions for each node provided by the HRS model. The conditions, namely, the release inventory, the pressure, and the temperature, were defined based on the values under normal operations for each node, as shown in Fig. 2. Release inventory, which dominates the amount of leaked hydrogen, is defined based on the maximum amount of hydrogen held by each node. In the present study, the release inventory for a certain node was defined as the total amount of hydrogen held by all equipment connected at the time of the release. However, it is assumed that the check valves are always effective at the time of release and that the total amount of released hydrogen is determined by the position of the check valves. Furthermore, it is assumed that the refueling operation is not conducted when the trailer is connected to an FCV, i.e., the trailer and the FCV are not connected at the same time. In the case that the release pressure is different from the hydrogen holding pressure for other equipment, the release inventory was calculated using the pressure condition at the leak point. The temperature at hydrogen release was defined as the internal temperature at each node. Although the hydrogen temperature in the dispenser node is approximately −40 °C, because of the pre-cooling system, the temperature is assumed to be 25 °C, which is the temperature in the cylinders, assuming that the pre-cooling system does not work at the flow rate at which hydrogen leaks. The pressure at which hydrogen is released was defined as the internal pressure at each node. Although there is a pressure distribution in the compressor node, the release pressure was assumed to be 82 MPa. The leak diameter was defined based on the inner diameter (6.3 mm) of the high-pressure pipe (82 MPa) carrying hydrogen and the inner diameter (50.5 mm) of the low-pressure pipe (0.6 MPa) carrying hydrogen. Sandia defined the cross-sectional area of five release holes (Rupture, Major, Medium, Minor, and Very Small) according to the cross-sectional area of Rupture (100%). We assumed that the inner diameter of the pipes is represented by the release hole size for all components, and we calculated the release hole sizes for all components.

The consequence analysis is conducted in three steps: discharge, dispersion, and flammable and explosive effect calculations. The leak rates, which are the results of discharge calculations, are also shown in Table 2. In addition, hazard zones for jet fires, flash fires, and VCEs were determined as flame envelopes and radiation heat flux contours, flame envelopes, and overpressure contours, respectively. We validated these consequence analysis results by comparing them to experimental results [18,19].

Table 3 shows the other conditions used in the consequence calculations. The weather conditions, Pasquill stability, wind speed, atmospheric temperature, relative humidity, and solar radiation flux were used to calculate the consequences. In order to obtain smooth risk contours, sixteen wind directions were selected. The height of hydrogen leakage was set to be 1 m, which is representative of the heights of leak holes. Note that the reference height was also set to 1 m from the ground, because the reference height has a greater effect on the consequence calculations near the leakage point, as is the case for an HRS, and the underestimation of the risk is prevented.

2.6. Impact assessment

Exposures to hydrogen flames, radiation heat flux, and overpressure due to an explosion can result in burn injury or lethality. We estimated the lethality using the criteria indicated in Purple Book [36] and the probit function suggested by Sandia [12]. The lethality of jet fires in the flame envelope was regarded as 100% and that outside of the flame was regarded as 100% when the radiation heat flux was over 35 kW/m^2, which is the value estimated by the proposed probit function when the radiation heat flux is under 35 kW/m^2. The lethality of flash fires in the flame envelope and outside of the flame was regarded as 100% and 0%, respectively. The lethality of VCEs was estimated using the proposed probit function.

3. Results and discussions

The IR of a scenario at an arbitrary point in the layout map was estimated by multiplying the frequency of occurrence of the

Table 2 – Process conditions for each node for consequence calculations.

Node		Inventory [m^3]	Temperature [°C]	Pressure [MPa]	Leak diameter [mm]		Leak rate [kg/s]	EFV working
Trailer	a-1	9.00	25	45	Very Small	0.063	0.000069	0
	a-2				Minor	0.20	0.00070	0
					Medium	0.63	0.0069	0
					Major	2.0	0.070	0
					Rupture	6.3	0.69	0
	b	9.01	25	45	Very Small	0.063	0.000069	0
					Minor	0.20	0.00070	0
					Medium	0.63	0.0069	0
					Major	2.0	0.070	0
					Rupture	6.3	0.69	0
	c	9.00	25	45	Very Small	0.063	0.000069	0
					Minor	0.20	0.00070	0
					Medium	0.63	0.0069	0
					Major	2.0	0.070	0
					Rupture	6.3	0.69	1
2-inch-pipe	a	788.40	25	45	Very Small	0.505	0.000074	0
					Minor	1.60	0.00074	0
					Medium	5.05	0.0074	0
					Major	16.0	0.074	0
					Rupture	50.5	0.74	1
Intermediate cylinders	a	9.00	25	45	Very Small	0.063	0.000069	0
					Minor	0.20	0.00070	0
					Medium	0.63	0.0069	0
					Major	2.0	0.070	0
					Rupture	6.3	0.69	1
	b	10.51	25	45	Very Small	0.063	0.000069	0
					Minor	0.20	0.00070	0
					Medium	0.63	0.0069	0
					Major	2.0	0.070	0
					Rupture	6.3	0.69	0
	C	10.51	25	45	Very Small	0.063	0.000069	0
					Minor	0.20	0.00070	0
					Medium	0.63	0.0069	0
					Major	2.0	0.070	0
					Rupture	6.3	0.69	1
	d	9.00	25	45	Very Small	0.063	0.000069	0
					Minor	0.20	0.00070	0
					Medium	0.63	0.0069	0
					Major	2.0	0.070	0
					Rupture	6.3	0.69	0
Compressor	a	5.77	25	45	Very Small	0.063	0.00012	0
	b				Minor	0.20	0.0012	0
	c				Medium	0.63	0.012	0
	d				Major	2.0	0.12	0
	e				Rupture	6.3	1.2	1
Cylinders	a	5.77	25	45	Very Small	0.063	0.00012	0
					Minor	0.20	0.0012	0
					Medium	0.63	0.012	0
					Major	2.0	0.12	0
					Rupture	6.3	1.2	1
	b-1	6.67	25	45	Very Small	0.063	0.00012	0
	b-2				Minor	0.20	0.0012	0
	b-3				Medium	0.63	0.012	0
					Major	2.0	0.12	0
					Rupture	6.3	1.2	0
	c-1	6.67	25	45	Very Small	0.063	0.00012	0
	c-2				Minor	0.20	0.0012	0
	c-3				Medium	0.63	0.012	0
	d				Major	2.0	0.12	0
					Rupture	6.3	1.2	1

(continued on next page)

Table 2 – (continued)

Node		Inventory [m^3]	Temperature [°C]	Pressure [MPa]	Leak diameter [mm]		Leak rate [kg/s]	EFV working
Dispenser	a	1.73	25	45	Very Small	0.063	0.00012	0
					Minor	0.20	0.0012	0
					Medium	0.63	0.012	0
					Major	2.0	0.12	0
					Rupture	6.3	1.2	1

Table 3 – Other conditions used in consequence calculations.

Pasquill stability	D	Relative humidity	0.7
Wind speed	1.5 m/s	Solar radiation flux	0.5 kW/m^2
Wind direction	16	Leak point height	1 m
Atmospheric temperature	9.85 °C	Reference height	1 m

scenario by the lethality of the scenario. Fig. 6 shows the risk contours of 10^{-3}, 10^{-4}, 10^{-5}, and 10^{-6} per year for the HRS model on the layout map. These contours indicate the summations of all of the risks from each node. The contours of 10^{-3} and 10^{-4} per year covered small areas near the leak points and were confined within the HRS boundaries. On the other hand, the contours of 10^{-5} and 10^{-6} per year covered almost the entire station and are not within the HRS boundaries. The longest distance that is from the north boundary of the station to the risk contour of 10^{-6} per year is approximately 10 m. Station personnel and customers inside the station could be exposed to the risks, greater than 10^{-3} per year. Thus, the risk is unacceptable compared with the risk acceptance criteria (10^{-4} per year) under the conditions of the present study model. Similarly, the acceptable IR criterion for a third party outside the station is 10^{-6} per year. Therefore, the risk is unacceptable compared to the criteria under the conditions of the present study model. However, note that, for the sake of the conservative evaluation, we made many assumptions, such as not considering the probability of station personnel and customers being present, using higher ignition probabilities, and using a model without the risk mitigation measures that have 3D structures. In addition, a sensitivity analysis focusing on the consequence calculation models and the modeling of safety equipment functions is conducted and provided in the Supporting Information.

In order to identify which nodes and scenarios has the greatest contribution to risk outside the station, we focused on the IRs on the RRPs we defined. Table 4 shows the risk values in Fig. 6 and their breakdown at the HRS boundary nearest each leakage point. The breakdown shows the nodes that have the top three risks with the highest contributions at each RRP and the scenarios that have the top three risks with the highest contributions at each node among many other scenarios that have risks. According to the breakdown of each scenario, it was found that almost all the risks at each RRP resulted in scenarios derived from the leakage from a compressor and cylinders, except for RRP "G", which is the nearest point to the dispenser. Risk ranking point "A", for example, has a total IR value of 3.3×10^{-6} per year, which is the most significant scenario and accounts for 7.57% of the total IR. This indicates hydrogen release from a pipe with a diameter of 6.3 mm (Rupture) based on instruments in the Cylinder (b-1) node for 12 s with gas/flame detection and auto shut-off valves. This is because the release is not stopped by the EFV. After all, the leakage point in the Cylinder (b-1) node is located upstream of the EFV inserted between the Cylinder (b-1) node and the Cylinder (c-1) node, although it is a rupture scenario that has a large amount of leakage.

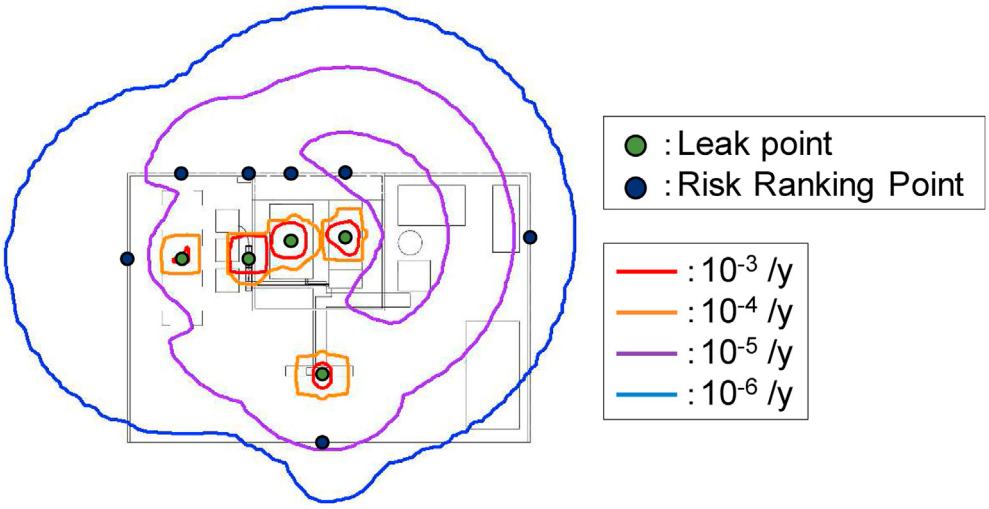

Fig. 6 – Individual risk contours in the HRS layout.

Table 4 – Summary of individual risks for each risk ranking point (RRP).

RRP	Coordinate	Total IR [/y]	Node	Component	Leak diameter	Scenario	Total IR [/y]	Ratio [–]
A	(0, 13.7)	3.3E-06	Cylinder (b-1)	Instrument	6.3 mm	Hydrogen release for 12 s with gas/fire detection and auto shut-off valves	2.52E-07	7.57
						Continuous release No rainout Immediate Horizontal Jet fire Only	2.29E-07	90.6
						Continuous release No rainout delayed Flash Fire Only	1.41E-08	5.61
						Continuous release No rainout delayed Flash Fire with explosion	9.53E-09	3.78
			Cylinder (b-2)	Instrument	6.3 mm	Hydrogen release for 12 s with gas/fire detection and auto shut-off valves	2.52E-07	7.57
						Continuous release No rainout Immediate Horizontal Jet fire Only	2.29E-07	90.6
						Continuous release No rainout delayed Flash Fire Only	1.41E-08	5.61
						Continuous release No rainout delayed Flash Fire with explosion	9.53E-09	3.78
			Cylinder (b-3)	Instrument	6.3 mm	Hydrogen release for 12 s with gas/fire detection and auto shut-off valves	2.52E-07	7.57
						Continuous release No rainout Immediate Horizontal Jet fire Only	2.29E-07	90.6
						Continuous release No rainout delayed Flash Fire Only	1.41E-08	5.61
						Continuous release No rainout delayed Flash Fire with explosion	9.53E-09	3.78
B	(4.1, 20)	1.3E-05	Cylinder (b-1)	Instrument	6.3 mm	Hydrogen release for 12 s with gas/fire detection and auto shut-off valves	1.34E-06	10.0
						Continuous release No rainout Immediate Horizontal Jet fire Only	1.32E-06	98.1
						Continuous release No rainout delayed Flash Fire Only	1.53E-08	1.14
						Continuous release No rainout delayed Flash Fire with explosion	1.02E-08	0.76
			Cylinder (b-2)	Instrument	6.3 mm	Hydrogen release for 12 s with gas/fire detection and auto shut-off valves	1.34E-06	10.0
						Continuous release No rainout Immediate Horizontal Jet fire Only	1.32E-06	98.1
						Continuous release No rainout delayed Flash Fire Only	1.53E-08	1.14
						Continuous release No rainout delayed Flash Fire with explosion	1.02E-08	0.76
			Cylinder (b-3)	Instrument	6.3 mm	Hydrogen release for 12 s with gas/fire detection and auto shut-off valves	1.34E-06	10.0
						Continuous release No rainout Immediate Horizontal Jet fire Only	1.32E-06	98.1
						Continuous release No rainout delayed Flash Fire Only	1.53E-08	1.14
						Continuous release No rainout delayed Flash Fire with explosion	1.02E-08	0.76
C	(9.05, 20)	2.1E-05	Compressor (c)	Filter	2.0 mm	Hydrogen release for 12 s with gas/fire detection and auto shut-off valves	1.52E-06	7.10
						Continuous release No rainout Immediate Horizontal Jet fire Only	1.52E-06	99.9
						Continuous release No rainout delayed Flash Fire Only	9.94E-10	0.07
						Continuous release No rainout delayed Flash Fire with explosion	6.66E-10	0.04
			Compressor (a)	Filter	2.0 mm	Hydrogen release for 12 s with gas/fire detection and auto shut-off valves	1.52E-06	7.10
						Continuous release No rainout Immediate Horizontal Jet fire Only	1.52E-06	99.9
						Continuous release No rainout delayed Flash Fire Only	9.94E-10	0.07
						Continuous release No rainout delayed Flash Fire with explosion	6.66E-10	0.04
			Cylinder (b-1)	Instrument	6.3 mm	Hydrogen release for 12 s with gas/fire detection and auto shut-off valves	1.36E-06	6.33
						Continuous release No rainout Immediate Horizontal Jet fire Only	1.33E-06	97.9
						Continuous release No rainout delayed Flash Fire Only	1.69E-08	1.25
						Continuous release No rainout delayed Flash Fire with explosion	1.13E-08	0.83
D	(12.2, 20)	1.7E-05	Compressor (c)	Filter	2.0 mm	Hydrogen release for 12 s with gas/fire detection and auto shut-off valves	3.47E-06	20.1
						Continuous release No rainout Immediate Horizontal Jet fire Only	3.46E-06	99.9
						Continuous release No rainout delayed Flash Fire Only	1.05E-09	0.03
						Continuous release No rainout delayed Flash Fire with explosion	7.05E-10	0.02
			Compressor (a)	Filter	2.0 mm	Hydrogen release for 12 s with gas/fire detection and auto shut-off valves	3.47E-06	20.1
						Continuous release No rainout Immediate Horizontal Jet fire Only	3.46E-06	99.9
						Continuous release No rainout delayed Flash Fire Only	1.05E-09	0.03
						Continuous release No rainout delayed Flash Fire with explosion	7.05E-10	0.02
			Intermediate cylinder (b)	Pipe	2.0 mm	Hydrogen release for 12 s with gas/fire detection and auto shut-off valves	1.08E-06	6.29

(*continued on next page*)

Table 4 – (*continued*)

RRP	Coordinate	Total IR [/y]	Node	Component	Leak diameter	Scenario	Total IR [/y]	Ratio [–]
						Continuous release No rainout Immediate Horizontal Jet fire Only	1.06E-06	98.2
						Continuous release No rainout delayed Flash Fire Only	1.11E-08	1.03
						Continuous release No rainout delayed Flash Fire with explosion	7.44E-09	0.69
E	(16.23, 20)	3.3E-06	Intermediate cylinder (b)	Valve	2.0 mm	Hydrogen release for 12 s with gas/fire detection and auto shut-off valves	2.62E-07	7.97
						Continuous release No rainout Immediate Horizontal Jet fire Only	2.62E-07	99.9
						Continuous release No rainout delayed Flash Fire Only	4.98E-11	0.02
						Continuous release No rainout delayed Flash Fire with explosion	3.34E-11	0.01
			Cylinder (b-1)	Valve	2.0 mm	Hydrogen release for 12 s with gas/fire detection and auto shut-off valves	2.50E-07	7.60
						Continuous release No rainout Immediate Horizontal Jet fire Only	2.49E-07	99.9
						Continuous release No rainout delayed Flash Fire Only	6.56E-11	0.03
						Continuous release No rainout delayed Flash Fire with explosion	4.39E-11	0.02
			Cylinder (b-2)	Valve	2.0 mm	Hydrogen release for 12 s with gas/fire detection and auto shut-off valves	2.50E-07	7.60
						Continuous release No rainout Immediate Horizontal Jet fire Only	2.49E-07	99.9
						Continuous release No rainout delayed Flash Fire Only	6.56E-11	0.03
						Continuous release No rainout delayed Flash Fire with explosion	4.39E-11	0.02
F	(30, 15.4)	7.8E-06	Cylinder (b-1)	Instrument	6.3 mm	Hydrogen release for 12 s with gas/fire detection and auto shut-off valves	1.21E-06	15.6
						Continuous release No rainout Immediate Horizontal Jet fire Only	1.19E-06	97.9
						Continuous release No rainout delayed Flash Fire Only	1.50E-08	1.24
						Continuous release No rainout delayed Flash Fire with explosion	1.01E-08	0.83
			Cylinder (b-2)	Instrument	6.3 mm	Hydrogen release for 12 s with gas/fire detection and auto shut-off valves	1.21E-06	15.6
						Continuous release No rainout Immediate Horizontal Jet fire Only	1.19E-06	97.9
						Continuous release No rainout delayed Flash Fire Only	1.50E-08	1.24
						Continuous release No rainout delayed Flash Fire with explosion	1.01E-08	0.83
			Cylinder (b-3)	Instrument	6.3 mm	Hydrogen release for 12 s with gas/fire detection and auto shut-off valves	1.21E-06	15.6
						Continuous release No rainout Immediate Horizontal Jet fire Only	1.19E-06	97.9
						Continuous release No rainout delayed Flash Fire Only	1.50E-08	1.24
						Continuous release No rainout delayed Flash Fire with explosion	1.01E-08	0.83
G	(14, 0)	1.4E-05	Dispenser (a)	Filter	2.0 mm	Hydrogen release for 12 s with gas/fire detection and auto shut-off valves	7.13E-06	49.6
						Continuous release No rainout Immediate Horizontal Jet fire Only	7.10E-06	99.5
						Continuous release No rainout delayed Flash Fire Only	2.00E-08	0.28
						Continuous release No rainout delayed Flash Fire with explosion	1.36E-08	0.20
			Cylinder (b-1)	Instrument	6.3 mm	Hydrogen release for 12 s with gas/fire detection and auto shut-off valves	7.49E-07	5.21
						Continuous release No rainout Immediate Horizontal Jet fire Only	7.21E-07	96.3
						Continuous release No rainout delayed Flash Fire Only	1.65E-09	2.20
						Continuous release No rainout delayed Flash Fire with explosion	1.11E-09	1.47
			Cylinder (b-2)	Instrument	6.3 mm	Hydrogen release for 12 s with gas/fire detection and auto shut-off valves	7.49E-07	5.21
						Continuous release No rainout Immediate Horizontal Jet fire Only	7.21E-07	96.3
						Continuous release No rainout delayed Flash Fire Only	1.65E-09	2.20
						Continuous release No rainout delayed Flash Fire with explosion	1.11E-09	1.47

As mentioned above, we found that the IRs at each RRP except for RRP "G" resulted in scenarios derived from the leakage from a compressor and cylinders, and the IRs at RRP "G" resulted in scenarios derived from the leakage from a dispenser. Zhiyong et al. [32] conducted a QRA of a gaseous HRS that is a 35 MPa station and showed that the compressor leak contributes 99% and 68% to the total IR of the two vulnerable spots inside the station. Zhiyong et al. [33] also conducted a QRA of another gaseous HRS that is a 35 MPa station and showed that leaks from compressors and dispensers contribute most risks to the two vulnerable spots inside the station. Although the location of RRPs is a little different between the past studies and our study, a comparison of these results can indicate that the leakage from cylinders emerges as the risks that contribute to the IRs at each RRP by increasing the hydrogen holding pressure to 82 MPa. On the other hand, Jafari et al. [43] conducted a QRA of a hydrogen generation unit using natural gas reforming process and showed that the heat exchanger and reformer have higher values of IR than the hydrogen purification absorber. A comparison of this result and our result may indicate that the most contributed risk of the IRs changes from the risk derived from hydrogen to the risk derived from other substances when hydrogen is replaced by other substances.

Looking at the breakdown in Table 4 in more detail, the release scenario of Cylinder node at RRP "A", for example, jet fire risk accounts for 90.6% of the total risk for the release scenario, and explosion and flash fire risk account for the remainder. In other words, the risk value for jet fire is approximately 10 times larger than that for explosion and flash fire. One of the main reasons for this is the impact assessments. The lethality of jet fires is defined whether an RRP is included in the flame envelope or not, and lethality of jet fire is regarded as 100% if the flame includes the RRP. On the other hand, the lethality of VCEs calculated in this assessment is approximately 0.1%, as estimated by the probit function. Thus, the difference was derived from this impact calculation. There are other factors, such as the assumption that the flame detection system takes 12 s to stop hydrogen leakage for the sake of a conservative evaluation, although it takes 2 s in reality, or the assumption that the immediate ignition probability is twice as large as the delayed ignition probability. However, these effects may be much smaller than the factor mentioned first. Other scenarios following the highest risk scenario, including the second and third scenarios, had the same trends. Therefore, the risk at RRP "A" was dominated by the jet fire risk derived from the Cylinder node.

The other RRPs had the same tendency, even if the risks derived from the nodes and components and the ratios of the risk values were slightly different. Thus it was found that all of the risks at each RRP were dominated by jet fire. At RRP "G", the most significant scenario is derived from the Dispenser (a) node and accounts for approximately half of the total risk. In addition, the ratio is much higher than for the other release scenarios. One of the main reasons for this is that the failure frequency for filters is much larger than those for the other components. Based on the above, we conclude that the risk of jet fire demonstrates the highest contribution to the risks at all of the risk ranking points and outside the station.

To reduce the risks and confine the risk contour of 10^{-6} per year within the Japanese HRS boundaries, it is necessary to consider risk mitigation measures to prevent jet fires. Such measures include shortening the release time to prevent continuous jet fires or the use of fire protection walls to reduce the radiation heat flux outside of the HRS. The HRS model in the present study does not take into account any 3D structures. Therefore, the risks of jet fires can be reduced by considering 3D structures, such as fire protection walls. Fire protection walls can be installed on the HRS boundaries, except on the public roadside (south side). As such, it is necessary to consider other safety measures for the south side (dispenser risk).

4. Conclusion

The purpose of the present study is to conduct a QRA of an HRS model representing Japanese HRSs to include the most current information and to identify the most significant scenarios that pose the greatest risks to the physical surroundings in the HRS model. We conducted a full QRA on the HRS model and obtained the IRs as risk contours. According to the results, the risk is unacceptable for station personnel and customers inside the station, as well as third parties outside the station, as compared with the risk acceptance criteria under the conditions of the present study model. However, note that we made many assumptions so as to evaluate the risks conservatively, such as not considering the existing probability of station personnel and customers, using higher ignition probabilities, or using a model without the risk mitigation measures that have 3D structures. Comparing the breakdown of the individual risks (IRs) at the risk ranking points, we conclude that the risk of jet fire demonstrates the highest contribution to the risks at all of the risk ranking points and outside the station. To reduce these risks and confine the risk contour of 10^{-6} per year within the HRS boundaries, it is necessary to consider risk mitigation measures for jet fires, such as shortening the release time to prevent from continuous jet fires or the use of fire protection walls to reduce the radiation heat flux outside of the HRS. The HRS model in the present study did not take into account any 3D structures. Therefore, the risks of jet fires can be reduced by considering the 3D structures, such as a fire protection wall. In the future, we intend to conduct a QRA taking into account a fire protection wall and to validate the effectiveness of this new analysis.

Declaration of competing interest

The authors declare that they have no known competing financial interests or personal relationships that could have appeared to influence the work reported in this paper.

Acknowledgment

This paper is based on results obtained from a project, JPNP18011, commissioned by the New Energy and Industrial Technology Development Organization (NEDO).

Appendix A. Supplementary data

Supplementary data to this article can be found online at https://doi.org/10.1016/j.ijhydene.2020.12.035.

REFERENCES

[1] Japanese Ministry of Economy, Trade and Industry, The Strategic Road Map for Hydrogen and Fuel Cells ~Industry-academia-government action plan to realize "Hydrogen Society", https://www.meti.go.jp/press/2018/03/20190312001/20190312001-3.pdf (accessed on 2. 2019.

[2] Cristina Galassi M, Papanikolaou Efthymia, Baraldi Daniele, Funnemark Espen, Haland Erling, Engebø Angunn, Haugom Gerd Petra, Jordan Avt Thomas. HIAD – hydrogen incident and accident database. Int J Hydrogen Energy 2012;37:17351–7.

[3] Løkke JA. The kjørbo incident. 2019. https://mb.cision.com/Public/115/2852735/8189422a0b076d6c.pdf.

[4] California Energy Commission. Failure modes and effects analysis for hydrogen fueling options. 2004.

[5] Messina MCFCLCMGCLG. Risk analysis of the storage unit in a hydrogen refuelling station. Int Conf Hydrog Saf n.d.:1–10.

[6] Casamirra M, Castiglia F, Giardina M, Lombardo C. Safety studies of a hydrogen refuelling station: determination of the occurrence frequency of the accidental scenarios. Int J Hydrogen Energy 2009;34:5846–54. https://doi.org/10.1016/j.ijhydene.2009.01.096.

[7] Pan X, Li Z, Zhang C, Lv H, Liu S, Ma J. Safety study of a wind–solar hybrid renewable hydrogen refuelling station in China. Int J Hydrogen Energy 2016;41:13315–21. https://doi.org/10.1016/j.ijhydene.2016.05.180.

[8] Kikukawa S, Yamaga F, Mitsuhashi H. Risk assessment of Hydrogen fueling stations for 70 MPa FCVs. Int J Hydrogen Energy 2008;33:7129–36. https://doi.org/10.1016/j.ijhydene.2008.08.063.

[9] Kikukawa S, Mitsuhashi H, Miyake A. Risk assessment for liquid hydrogen fueling stations. Int J Hydrogen Energy 2009;34:1135–41. https://doi.org/10.1016/j.ijhydene.2008.10.093.

[10] Nakayama J, Sakamoto J, Kasai N, Shibutani T, Miyake A. Preliminary hazard identification for qualitative risk assessment on a hybrid gasoline-hydrogen fueling station with an on-site hydrogen production system using organic chemical hydride. Int J Hydrogen Energy 2016;41:7518–25. https://doi.org/10.1016/j.ijhydene.2016.03.143.

[11] LaChance J, Houf W, Middleton B, Fluer L. Analyses to support development of risk-informed separation distances for hydrogen codes and standards. Sandia Rep SAND2009 2009. ….

[12] Groth Katrina MESH. Methodology for assessing the safety of hydrogen systems: HyRAM 1.1 technical reference manual. 2017. SAND2017-2998.

[13] Tsunemi K, Yoshida K, Kihara T, Saburi T, Ono K. Screening-level risk assessment of a hydrogen refueling station that uses organic hydride. Sustain Times 2018;10. https://doi.org/10.3390/su10124477.

[14] Pasman HJ, Rogers WJ. Risk assessment by means of Bayesian networks: a comparative study of compressed and liquefied H 2 transportation and tank station risks. Int J Hydrogen Energy 2012;37:17415–25. https://doi.org/10.1016/j.ijhydene.2012.04.051.

[15] Chang Y, Zhang C, Shi J, Li J, Zhang S, Chen G. Dynamic Bayesian network based approach for risk analysis of hydrogen generation unit leakage. Int J Hydrogen Energy 2019;44:26665–78. https://doi.org/10.1016/j.ijhydene.2019.08.065.

[16] Castiglia F, Giardina M. Analysis of operator human errors in hydrogen refuelling stations: comparison between human rate assessment techniques. Int J Hydrogen Energy 2013;38:1166–76. https://doi.org/10.1016/j.ijhydene.2012.10.092.

[17] Venetsanos AG, Huld T, Adams P, Bartzis JG. Source, dispersion and combustion modelling of an accidental release of hydrogen in an urban environment. J Hazard Mater 2003;105:1–25. https://doi.org/10.1016/j.jhazmat.2003.05.001.

[18] Takeno K, Okabayashi K, Kouchi A, Nonaka T, Hashiguchi K, Chitose K. Dispersion and explosion field tests for 40 MPa pressurized hydrogen. Int J Hydrogen Energy 2007;32:2144–53. https://doi.org/10.1016/j.ijhydene.2007.04.018.

[19] Mogi T, Horiguchi S. Experimental study on the hazards of high-pressure hydrogen jet diffusion flames. J Loss Prev Process Ind 2009;22:45–51. https://doi.org/10.1016/j.jlp.2008.08.006.

[20] Dadashzadeh M, Ahmad A, Khan F. Dispersion modelling and analysis of hydrogen fuel gas released in an enclosed area: a CFD-based approach. Fuel 2016;184:192–201. https://doi.org/10.1016/j.fuel.2016.07.008.

[21] Kim E, Park J, Cho JH, Moon I. Simulation of hydrogen leak and explosion for the safety design of hydrogen fueling station in Korea. Int J Hydrogen Energy 2013;38:1737–43. https://doi.org/10.1016/j.ijhydene.2012.08.079.

[22] Proust C, Jamois D, Studer E. High pressure hydrogen fires. Int J Hydrogen Energy 2011;36:2367–73. https://doi.org/10.1016/j.ijhydene.2010.04.055.

[23] Shirvill LC, Roberts TA, Royle M, Willoughby DB, Gautier T. Safety studies on high-pressure hydrogen vehicle refuelling stations: releases into a simulated high-pressure dispensing area. Int J Hydrogen Energy 2012;37:6949–64. https://doi.org/10.1016/j.ijhydene.2012.01.030.

[24] Schefer RW, Merilo EG, Groethe MA, Houf WG. Experimental investigation of hydrogen jet fire mitigation by barrier walls. Int J Hydrogen Energy 2011;36:2530–7. https://doi.org/10.1016/j.ijhydene.2010.04.008.

[25] Sathiah P, Dixon CM. Numerical modelling of release of subsonic and sonic hydrogen jets. Int J Hydrogen Energy 2019;44:8842–55. https://doi.org/10.1016/j.ijhydene.2018.09.182.

[26] Industries MH. Characteristics and safety for open-jet flame of high-pressurized hydrogen. J Combust Soc Japan 2010;52:121–9. https://doi.org/10.20619/jcombsj.52.160_121.

[27] Cirrone DMC, Makarov D, Molkov V. Thermal radiation from cryogenic hydrogen jet fires. Int J Hydrogen Energy 2019;44:8874–85. https://doi.org/10.1016/j.ijhydene.2018.08.107.

[28] Kikukawa S. Consequence analysis and safety verification of hydrogen fueling stations using CFD simulation. Int J Hydrogen Energy 2008;33:1425–34. https://doi.org/10.1016/j.ijhydene.2007.11.027.

[29] Matthijsen AJCM, Kooi ES. Safety distances for hydrogen filling stations. J Loss Prev Process Ind 2006;19:719–23. https://doi.org/10.1016/j.jlp.2006.05.006.

[30] LaChance J. Risk-informed separation distances for hydrogen refueling stations. Int J Hydrogen Energy 2009;34:5838–45. https://doi.org/10.1016/j.ijhydene.2009.02.070.
[31] LaChance J, Tchouvelev A, Ohi J. Risk-informed process and tools for permitting hydrogen fueling stations. Int J Hydrogen Energy 2009;34:5855–61. https://doi.org/10.1016/j.ijhydene.2009.01.057.
[32] Zhiyong L, Xiangmin P, Jianxin M. Quantitative risk assessment on a gaseous hydrogen refueling station in Shanghai. Int J Hydrogen Energy 2010;35:6822–9. https://doi.org/10.1016/j.ijhydene.2010.04.031.
[33] Zhiyong L, Xiangmin P, Jianxin M. Quantitative risk assessment on 2010 Expo hydrogen station. Int J Hydrogen Energy 2011;36:4079–86. https://doi.org/10.1016/j.ijhydene.2010.12.068.
[34] Gye HR, Seo SK, Bach QV, Ha D, Lee CJ. Quantitative risk assessment of an urban hydrogen refueling station. Int J Hydrogen Energy 2019;44:1288–98. https://doi.org/10.1016/j.ijhydene.2018.11.035.
[35] Ccps. Guidelines for chemical process quantitative risk analysis. 2nd ed. 2000.
[36] Van Ryzin J. Guidelines for Quantitative risk assessment. [CPR 18E]. Purple B 1980;22:321–6.
[37] DNV. Main report – survey of hydrogen risk assessment methods. Assessment 2008.
[38] Ham K, Marangon A, Middha P, Versloot N, Rosmuller N, Carcassi M, et al. Benchmark exercise on risk assessment methods applied to a virtual hydrogen refuelling station. Int J Hydrogen Energy 2011;36:2666–77. https://doi.org/10.1016/j.ijhydene.2010.04.118.
[39] ISO 19880-1. Gaseous hydrogen -fuelling stations-, Part 1: general requirements. 2020.
[40] Tsunemi K, Kihara T, Kato E, Kawamoto A, Saburi T. Quantitative risk assessment of the interior of a hydrogen refueling station considering safety barrier systems. Int J Hydrogen Energy 2019;44:23522–31. https://doi.org/10.1016/j.ijhydene.2019.07.027.
[41] Japan Nuclear Safety Institute. JANSI-CFR-02, Estimation of domestic general equipment failure rate considering uncertainty of the number of failures. 2016 (in Japanese).
[42] OREDA. Oreda (Offshore & onshore reliability data) handbook. 6th ed., vol. 1; 2015.
[43] Jafari MJ, Zarei E, Badri N. The quantitative risk assessment of a hydrogen generation unit. Int J Hydrogen Energy 2012;37. https://doi.org/10.1016/j.ijhydene.2012.09.082. 19241–9.